arXiv:cond-mat/0005376v2 [cond-mat.mtrl-sci] 28 Aug 2000

Asymptotic step profiles from a nonlinear growth equation for vicinal surfaces

Jouni Kallunki and Joachim Krug
Fachbereich Physik, Universität GH Essen, 45117 Essen, Germany
(February 1, 2008)

We study a recently proposed nonlinear evolution equation describing the collective step meander on a vicinal surface subject to the Bales-Zangwill growth instability [O. Pierre-Louis *et al.*, Phys. Rev. Lett. **80**, 4221 (1998)]. A careful numerical analysis shows that the dynamically selected step profile consists of sloped segments, given by an inverse error function and steepening as $\sqrt{t}$, which are matched to pieces of a stationary (time-independent) solution describing the maxima and minima. The effect of smoothening by step edge diffusion is included heuristically, and a one-parameter family of evolution equations is introduced which contains relaxation by step edge diffusion and by attachment-detachment as special cases. The question of the persistence of an initially imposed meander wavelength is investigated in relation to recent experiments.

05.70.Ln, 81.10.Aj, 68.35.Bs

I. INTRODUCTION

Ten years ago, Bales and Zangwill [1] predicted that a growing vicinal surface should undergo a step meandering instability when kinetic step edge barriers suppress the attachment of atoms to descending steps [2]. The instability has meanwhile been observed in experiments [3,4] and Monte Carlo simulations [5], and a number of theoretical studies have been devoted to the nonlinear evolution of the surface both in the presence [6] and absence [5,7] of desorption [8].

Since linear stability analysis shows the in-phase mode of the collective step meander to be the most unstable [9], the two-dimensional surface morphology can be represented by a one-dimensional function $\zeta(x,t)$ describing the displacement of the common step profile from the flat straight reference configuration $\zeta = 0$, with the x-axis oriented along the step [10]. For the case of infinite step edge barriers, attachment-detachment kinetics and no desorption, the nonlinear evolution equation

$$\zeta_t = -\left\{ \frac{\alpha\zeta_x}{1+\zeta_x^2} + \frac{\beta}{1+\zeta_x^2}\left[\frac{\zeta_{xx}}{(1+\zeta_x^2)^{3/2}}\right]_x \right\}_x \qquad (1)$$

was proposed in Ref. [7] (subscripts denote derivatives). It can be derived from the Burton-Cabrera-Frank (BCF) theory of growth on vicinal surfaces [11] using a singular multiscale expansion [7,12] in $\epsilon^{1/2}$, where $\epsilon = \Omega F\ell^2/D$ is the Péclet number. Here F is the deposition flux, D the in-plane surface diffusion coefficient, ℓ the nominal step spacing, and Ω the atomic area. The coefficients in Eq.(1) are given by $\alpha = \Omega F\ell^2/2$ and $\beta = \Omega^2 D\ell\gamma c_{\rm eq}/k_BT$, with γ and $c_{\rm eq}$ referring to the step stiffness and the equilibrium adatom density, respectively.

According to (1), the straight step is linearly unstable against perturbations with wavelengths larger than $\lambda_c = 2\pi\sqrt{\beta/\alpha}$, with a fastest growing wavelength $\lambda_u = \sqrt{2}\lambda_c$. To explore the nonlinear regime, in Ref. [7] a numerical integration of Eq.(1) was carried out which showed an increase of the meander amplitude as $\sqrt{t}$ at fixed wavelength λ_u, as well as the formation of spike singularities at maxima and minima of ζ. The latter is surprising because the second term on the right hand side of (1) would be expected to suppress such rapid variations of the step curvature.

Here we revisit the problem using a more accurate numerical algorithm [13]. We demonstrate that the step profile remains smooth near maxima and minima, where it approaches asymptotically a *stationary* (time-independent) solution of (1), while the sides of the profile follow a separable solution with an amplitude of order $\sqrt{t}$. The matching of the two solutions occurs near the point of maximum slope. We further show heuristically how the effect of step edge diffusion can be included in the theory, and introduce a generalized evolution equation which contains edge diffusion and attachment-detachment kinetics as special cases. Finally, we address the question to what extent an initially imposed meander wavelength different from λ_u is preserved under the time evolution. This is relevant in view of the recent experiments of Maroutian *et al.* [4].

II. SHAPE SELECTION

Before presenting the numerical results we recapitulate the two classes of analytic solutions to (1) which were found in [7]. *Stationary* solutions are obtained by setting the mass current along the step (the quantity inside to curly brackets on the right hand side of (1)) to zero. In terms of $m(x) = \zeta_x/\sqrt{1+\zeta_x^2}$ the stationarity condition reduces to Newton's equation $\beta d^2m/dx^2 = -dU/dm$ for a classical particle of mass β moving in the potential $U(m) = -\alpha\sqrt{1-m^2}$, which can be solved by quadratures. One thus obtains a one-parameter family of periodic profiles $\zeta_S(x)$ which are most conveniently parameterized by the maximum slope $S \equiv \max_x \zeta_x$, and which have been described previously in the context of a different surface evolution equation [15]. The amplitude $A(S)$

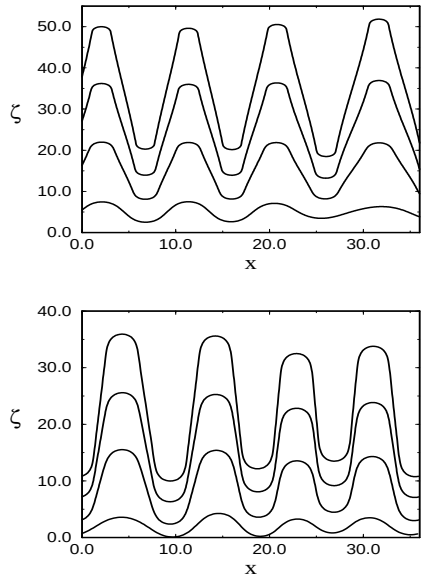

FIG. 1. The evolution of the step profile starting from a flat initial condition with small random fluctuations. The upper figure shows the case of attachment-detachment kinetics (Eq.(1)) at times $t = 36, 64, 110, 183$, the lower figure the case of edge diffusion (Eq.(4) with $n = 1/2$) at times $t = 20, 60, 112, 200$. Subsequent profiles have been shifted in the ζ-direction. In all figures spatial variables have been scaled by $\lambda_c/2\pi = \sqrt{\beta/\alpha}$ and time by β/α^2.

is an increasing function of S, while the wavelength $\Lambda(S)$ decreases with increasing S, starting out at $\Lambda(0) = \lambda_c$. For $S \to \infty$ finite limiting values $A(\infty) = \sqrt{8\beta/\alpha}$, $\Lambda(\infty) = \sqrt{2\pi\beta/\alpha}\ \Gamma(3/4)/\Gamma(5/4) \approx 0.5393527..\lambda_c$ are approached.

The *separable* solution of interest reads [7,14]

$$\zeta(x,t) = 2\sqrt{\alpha t}\ \mathrm{erf}^{-1}\left(1 - 4|x|/\lambda_s\right), \qquad (2)$$

$-\lambda_s/2 < x < \lambda_s/2$, where $\mathrm{erf}(z) = (2/\sqrt{\pi})\int_0^z dy\ e^{-y^2}$, and the wavelength λ_s is arbitrary. Equation (2) solves (1) exactly in the limit $t \to \infty$, when the second term on the right hand side becomes negligible compared to the first, and the evolution equation reduces to $\zeta_t = -(\alpha/\zeta_x)_x$. The solution (2) is singular near the maxima and minima, where it diverges as $\zeta \sim \pm\sqrt{\ln(1/|x - x_0|)}$, $x_0 = 0, \pm\lambda_s/2$.

In Figure 1 we show results of a numerical solution of (1), starting from a small amplitude random initial condition. To secure good numerical stability we used a fully implicit, backwards Euler algorithm for integration. The algorithm was implemented on an adaptive grid in order to obtain sufficient lateral resolution at the singular points.

A regular meander pattern of wavelength λ_u develops, with an amplitude growing indefinitely as $\sqrt{t}$. Closer inspection reveals that the sides of the profile follow the separable solution (Figure 2), while near the maxima and minima smooth *caps* appear which approach pieces of the

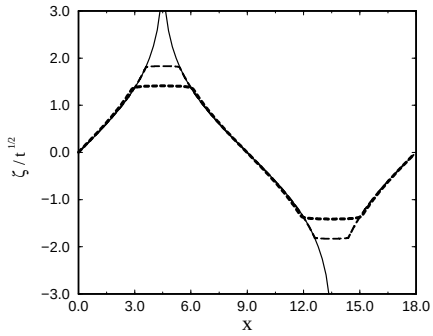

FIG. 2. The asymptotic form of the scaled profile $\zeta/\sqrt{t}$ for Eq.(1) (long dashes) and Eq.(4) with $n = 1/2$ (short dashes). Full line is the separable solution (2) with λ_s equal to the total meander wavelength $\lambda = 18\sqrt{\beta/\alpha} \approx 2\lambda_u$.

stationary solutions (Figure 3). This can be understood by noting that the mass current along the sides of the profile vanishes as $1/\sqrt{t}$ according to (2), and therefore the stationarity condition is asymptotically satisfied; we have checked that the deviation from the stationary profile which is discernible in Figure 3 vanishes as $1/\sqrt{t}$. Since the slope of (2) increases monotonically upon approaching an extremum while it decreases for the stationary profiles, the matching of the two solutions occurs near the point of maximum slope. For $t \to \infty$ the slope of the separable solution diverges, hence the cap profile approaches the limiting stationary solution $\zeta_\infty(x)$, and the length of the cap becomes $\Lambda(\infty)/2$. The rescaled step profile $\zeta(x,t)/\sqrt{t}$ approaches an invariant shape in which the cap appears as a flat facet. The wavelength λ_s of the separable solution depends on the cap length and on the total meander wavelength λ, and is fixed by mass balance requirements [12]; for large total wavelength $\lambda_s \to \lambda$ (see Figure 2).

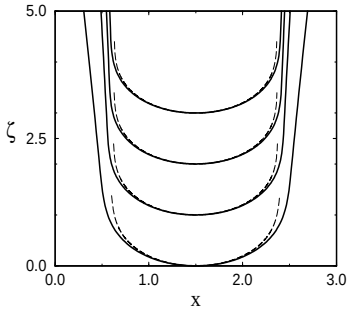

FIG. 3. The form of the caps for Eq.(1) at $t = 500, 1500, 2500, 3400$. The dashed lines are the stationary solutions corresponding to the maximum slope in the profile.

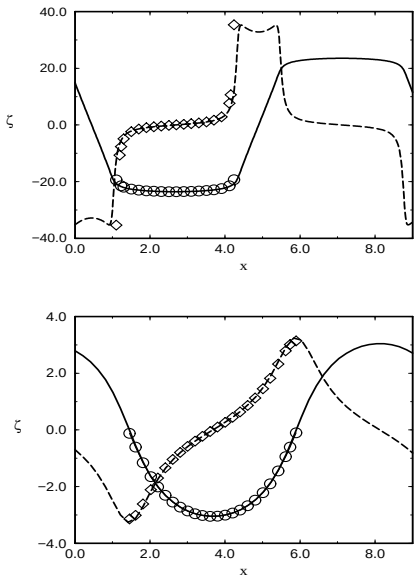

FIG. 4. Asymptotic form of the step profile for $n = 1/2$ (upper) and $n = 0$ (lower). Full line is the profile and dashed line the slope ζ_x. Circles represent the stationary solution and diamonds the corresponding slope. The separable solution, still present in the sloped regions of the profile for $n = 1/2$, has vanished for $n = 0$.

III. STEP EDGE DIFFUSION AND A GENERALIZED EVOLUTION EQUATION

On many fcc metal surfaces, diffusion along step edges is the fastest kinetic process which therefore provides the dominant step smoothening mechanism [16]. To see how Eq.(1) has to be modified to take this effect into account, we note first that the second, relaxational term on the right hand side can be rewritten in a geometrically covariant form as $(\sigma\mu_s)_x$, where $\mu = \Omega\gamma\kappa$ is the step chemical potential [16], $\kappa = -(1+\zeta_x^2)^{-3/2}\zeta_{xx}$ is the step curvature, $s = \int dx\ \sqrt{1+\zeta_x^2}$ is the arclength along the step, and

$$\sigma = \frac{D\Omega c_{\rm eq}}{k_B T}\frac{\ell}{\sqrt{1+\zeta_x^2}} \tag{3}$$

is a mobility. The ℓ-dependence in (3) reflects the assumed relaxation kinetics [7], in which mass exchange between different parts of the step occurs through detachment followed by diffusion over the terrace, reflection at the descending step, and re-attachment (case E of [18]). The factor $1/\sqrt{1+\zeta_x^2}$ has a simple geometric interpretation [17]: For a deformed in-phase step train the distance to the nearest step, measured along the step normal, is $\ell/\sqrt{1+\zeta_x^2}$ rather than ℓ.

For relaxation through step edge diffusion the mobility is clearly independent of the step distance, and is given by [18] $\tilde\sigma = D_{\rm e}\Omega c_{\rm e}/k_B T$, where $D_{\rm e}$ and $c_{\rm e}$ denote the edge diffusion coefficient and the equilibrium concentration of edge atoms, respectively. When edge diffusion dominates (i.e. $\tilde\sigma \gg \sigma$), the appropriate nonlinear growth equation should thus be given by (1) with the second term replaced by $(\tilde\sigma\mu_s)_x = ([1+\zeta_x^2]^{-1/2}\tilde\sigma\mu_x)_x$. This is confirmed by the explicit derivation of Gillet *et al.* [12], who also studied the crossover between attachment-detachment kinetics and edge diffusion. Here our primary goal is to gain further insight into the shape selection mechanism. This has lead us to consider the generalized class of equations

$$\zeta_t = -\left\{\frac{\alpha\zeta_x}{1+\zeta_x^2} + \frac{\beta}{(1+\zeta_x^2)^n}\left[\frac{\zeta_{xx}}{(1+\zeta_x^2)^{3/2}}\right]_x\right\}_x, \tag{4}$$

which reduces to (1) for $n = 1$ and describes relaxation through step edge diffusion when $n = 1/2$ and $\beta = \Omega^2 D_{\rm e} c_{\rm e}\gamma/k_B T$. Below we discuss the properties of (4) for general n, keeping in mind that the cases $n = 1/2$ and $n = 1$ are of immediate physical relevance.

The separable solution (2) becomes exact in a limit where the relaxation term in (1) can be neglected, hence it remains a valid asymptotic solution also of (4) for $n > -1/2$; for $n \le -1/2$ the relaxation term can never be ignored. The stationary solutions of (4) can be analyzed in terms of the same mechanical analogy described above, the particle potential being given by $U(m) = -\alpha(1-m^2)^{3/2-n}/(3-2n)$. For $1/2 < n < 3/2$ the behavior is analogous to that for $n = 1$: The wavelength $\Lambda(S)$ is a decreasing function of the maximal slope S, and wavelength and amplitude reach finite values $A(\infty) = \sqrt{8\beta/\alpha}\sqrt{3-2n}/(2n-1)$ and

$$\Lambda(\infty) = \sqrt{2\pi(3-2n)(\beta/\alpha)}\frac{\Gamma[(2n+1)/4]}{\Gamma[(2n+3)/4]} \tag{5}$$

for $S \to \infty$. Thus the asymptotic step profiles look similar to those generated by Eq.(1), with the length of the cap decreasing with increasing n. As $n \to 3/2$ the cap length, given by $\Lambda(\infty)/2$, vanishes. For $n \ge 3/2$ we therefore expect true spike singularities to develop at the maxima and minima of the profile. Using that the slope imposed by the separable solution (2) grows as $S \sim \sqrt{t}$, we predict that the curvature at the extrema diverges as $t^{(2n-3)/4}$.

A numerical solution for the case of edge diffusion ($n = 1/2$) is shown in the lower panel of Figure 1. For $n = 1/2$ the potential $U(m)$ is harmonic and hence the wavelength $\Lambda(S) = \lambda_c$ independent of S. The amplitude of the stationary profiles diverges as $A(S) \sim \ln S$, leading to a corresponding increase of the cap height as $\ln t$. Since this is still small compared to the overall profile amplitude, the caps nevertheless appear as flat in the rescaled shape $\zeta/\sqrt{t}$ (Figure 2; a detailed view of the cap is shown in Figure 4). This remains true in the entire interval $-1/2 < n \le 1/2$, where the cap length (5) remains finite and the cap height grows as $t^{(1-2n)/4}$. However a qualitative change in the profile evolution occurs at the value $n_c \approx 0.2283$ where the asymptotic stationary wavelength (5) becomes equal to the most unstable wavelength λ_u, which sets the lateral length scale in the

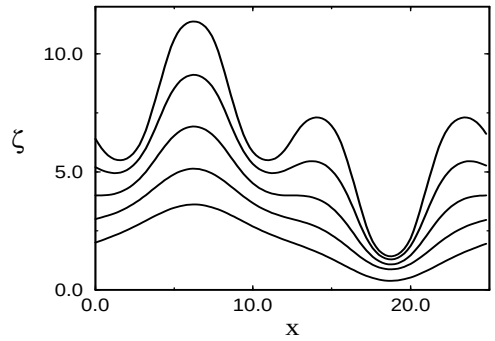

FIG. 5. Spontaneous creation of an extra meander period for the case of step-edge diffusion ($n = 1/2$). The initial wavelength of the profile is $\lambda_i = 25\sqrt{\beta/\alpha} > 3\lambda_c$.

early stages of growth. For $n < n_c$ we expect to see an intermediate *coarsening* regime in which the lateral length scale increases from λ_u to $\Lambda(\infty)$. Coarsening to arbitrarily large length scales, similar to what is observed in related evolution equations for one-dimensional unstable growth [19], sets in at $n = -1/2$, where (5) diverges. Throughout the regime $n < n_c$ the evolving profile is describable in terms of stationary solutions, and the separable solution (2) no longer plays any role (Figure 4).

IV. PERSISTENCE OF THE INITIAL WAVELENGTH

Finally, we address the recent experiments [4] on surfaces vicinal to Cu(100), in which the meander wavelength was measured as a function of temperature, and it was concluded that the observed behavior is *inconsistent* with the theoretical prediction for the linearly most unstable wavelength λ_u. Maroutian *et al.* [4] therefore proposed that the meander wavelength is set by the *nucleation length* describing the distance between the one-dimensional nuclei appearing on a flat step in the early stage of growth, which can be considerably larger than λ_u.

A necessary consistency requirement for this scenario is that an initially imposed meander wavelength $\lambda_i > \lambda_u$ persists during the nonlinear evolution. We have therefore numerically integrated Eqs.(1, 4) starting from a sinusoidal initial condition with varying wavelength λ_i. We do find that a range of wavelengths can be preserved during growth. This is reasonable in view of the analysis presented above, which shows that asymptotic profiles, composed of the separable solution (2) and a stationary cap, can in principle be constructed for arbitrary wavelength (see e.g. Figure 2). However, when λ_i exceeds λ_c by more than a factor of 3, so that an additional meander fits between the maxima and minima of the profile, the wavelength spontaneously decreases to a value near λ_u (Figure 5). This result contradicts the assumption of [4] that initial wavelengths much larger than λ_u persist, but it should not be overemphasized: Clearly processes which involve a change in the collective meander wavelength may not be accurately described in a model which assumes in-phase meandering from the outset.

V. OUTLOOK

In conclusion, we have described an unusual shape selection scenario for a class of physically motivated growth equations. A number of issues remain to be clarified. Mathematically, the behavior in the region where separable and stationary solutions match needs further investigation; our numerical work indicates the appearance of singularities in higher derivatives of ζ. Also the dynamics in the singular regime $n \geq 3/2$ and in the coarsening regime $n < n_c$ of Eq.(4) deserves attention. Physically, it is imperative that the predictions of the one-dimensional equations for the in-phase step meander be confirmed by more complete descriptions of the growing surface, as provided by two-dimensional continuum equations and Monte Carlo models [5], in order to assess their ultimate relevance for the experimentally observed morphologies.

ACKNOWLEDGEMENTS

We are much indebted to Jens Eggers for help with the numerical algorithm and useful discussions. Olivier Pierre-Louis and Chaouqi Misbah kindly supplied us with a copy of [12] prior to publication. Support by DFG/SFB 237 is gratefully acknowledged.

[1] G. S. Bales and A. Zangwill, Phys. Rev. B **41**, 5500 (1990).
[2] R.L. Schwoebel and E.J. Shipsey, J. Appl. Phys. **37**, 3682 (1966).
[3] L. Schwenger, R.L. Folkerts and H.-J. Ernst, Phys. Rev. B **55**, R7406 (1997); J.E. Van Nostrand, S.J. Chey and D.G. Cahill, Phys. Rev. B **57**, 12536 (1998); P. Tejedor, P. Šmilauer and B.A. Joyce, Microelectronics Journal **30**, 477 (1999).
[4] T. Maroutian, L. Duillard and H.-J. Ernst, Phys. Rev. Lett. **83**, 4353 (1999).
[5] M. Rost, P. Šmilauer and J. Krug, Surf. Sci. **369**, 393 (1996).
[6] O. Pierre-Louis and C. Misbah, Phys. Rev. B **58**, 2259 (1998); *ibid.* 2276 (1998).
[7] O. Pierre-Louis, C. Misbah, Y. Saito, J. Krug and P. Politi, Phys. Rev. Lett. **80**, 4221 (1998).
[8] For a review, see P. Politi, G. Grenet, A. Marty, A. Ponchet and J. Villain, Phys. Rep. **324**, 271 (2000).

[9] A. Pimpinelli, I. Elkinani, A. Karma, C. Misbah and J. Villain, J. Phys.: Condens. Matter **6**, 2661 (1994).
[10] This entails the simplifying assumption of long-range phase coherence. In fact topological defects in the meandering pattern appear in the early stages of growth, see [5].
[11] W.K. Burton, N. Cabrera and F.C. Frank, Philos. Trans. R. Soc. London A **243**, 299 (1951).
[12] F. Gillet, O. Pierre-Louis and C. Misbah (preprint; cond-mat/0005422).
[13] An independent numerical investigation was carried out in Ref. [12]. Their conclusions agree with ours.
[14] J. Krug, J. Stat. Phys. **87**, 505 (1997).
[15] D.J. Srolovitz, A. Mazor and B.G. Bukiet, J. Vac. Sci. Technol. A **6**, 2371 (1988).
[16] H.-C. Jeong and E.D. Williams, Surf. Sci. Reports **34**, 171 (1999).
[17] J. Krug, Physica A **263**, 174 (1999).
[18] A. Pimpinelli, J. Villain, D. E. Wolf J. J. Métois, J. C. Heyraud, I. Elkiani and G. Uimin, Surf. Sci. **295**, 143 (1993).
[19] P. Politi and A. Torcini, J. Phys. A **33**, L77 (2000).